HVAC&R Research

Publication details, including instructions for authors and subscription information:
http://www.tandfonline.com/loi/uhvc20

Simplified Model for the Operation of Chilled Water Cooling Coils Under Nonnominal Conditions

O. Morisot [a] , D. Marchio [b] & P. Stabat [c]

[a] ELYO Cylergie, France

[b] Centre of Energy Studies, Ecole des Mines de Paris, France

[c] Centre of Energy Studies, Ecole des Mines de Paris

Published online: 28 Feb 2011.

Simplified Model for the Operation of Chilled Water Cooling Coils Under Nonnominal Conditions

O. Morisot, Ph.D. **D. Marchio, Ph.D.** **P. Stabat**
Student Member ASHRAE

This study presents a cooling coil model for calculating energy consumption in air-conditioned buildings that has a minimal number of inputs. The model accurately determines the cooling energy rate and dehumidification energy rate under nonnominal conditions, and takes into account operation under variable air and water flows. In this manner, the model enhances the simplified ASHRAE Toolkit *model without requiring more input data. The main assumptions are justified considering the common existing configurations of cooling coils in the air-conditioning industry. The parameters of the model are identified from only one nominal rating point. The model has been validated on a VAV facility with an average deviation of 5% for total energy rate. Errors are mainly due to the assumption that the coil is either completely wet or dry even if the surface is partially wet.*

INTRODUCTION

One of the important models needed for estimating energy consumption of HVAC system is a cooling coil model suitable for both cooling and dehumidification. HVAC systems very often operate using only temperature control. The load induced by noncontrolled dehumidification is not negligible compared to the yearly energy consumption and needs to be calculated. Building indoor air humidity has to be predicted under nonnominal conditions. Moreover, the coil model has to take into account the effect of variable air and water flows on heat transfer to accurately compare the performance of various HVAC systems [e.g., Constant Air Volume (CAV) and Variable Air Volume (VAV) systems, and variable speed pumps]. Moreover, the simplified model operating under nonnominal conditions allows the production of training data for artificial neural networks used in the field of fault detection and diagnosis method applied to building air-conditioning.

Existing models of cooling coils do not meet the following requirements for the building energy consumption simulation:

- Coil characteristics determination using available data (the performance at a single rating point is often the only piece of information given in catalogs by manufacturers)
- Dehumidification energy rate calculation under nonrating conditions
- Adaptability to variable airflow rate (VAV systems)
- Adaptability to variable water flow rate (water flow control devices or variable-speed pumps)

In this paper, a cooling coil model is developed based on the ASHRAE *HVAC 2 Toolkit* simplified cooling coil model (Brandemuehl et al. 1993). The coil is modeled as a classical

Olivier Morisot in an engineer in energy and the environment at ELYO Cylergie, France. **Dominique Marchio** is a professor at the Centre of Energy Studies, Ecole des Mines de Paris, France. **Pascal Stabat** is a doctoral student at the Centre of Energy Studies, Ecole des Mines de Paris.

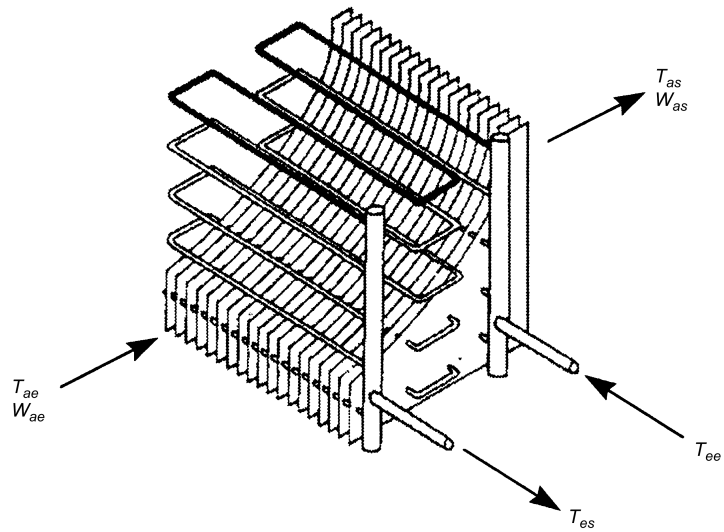

Figure 1. Cooling Coil Representation for Building Air Conditioning
(Holmes 1988)

counterflow heat exchanger suitable for building air-conditioning with fins in counterflow configuration or in crossflow configuration with at least four rows, as illustrated in Figure 1.

COOLING COIL MODEL

Local and Global Heat and Mass Transfer Exchange

In the cooling coil, there is a sensible thermal exchange between air and cooling fluid flowing through the pipes. When the pipe surface temperature is below the air dew-point temperature, a mass exchange occurs as illustrated in Figure 2. To analyze the airside heat transfer and mass transfer, the following assumptions are made:

- Air and water are considered homogeneous outside the thermal and diffusion boundary layer
- Conduction heat transfer in material is negligible compared to convection heat transfer
- Air condensation film is assumed to be saturated air at film temperature T_{cond}

The total energy exchanged by the air over an incremental pipe surface (dA) can be expressed with the convection coefficient h_{ext} between the air and pipe surface and the mass transfer coefficient h_{mass},

$$dQ = h_{ext} dA(T_a - T_{cond}) + h_{mas} dA[w_a(H_{fg} + c_{pv}T_a) - w_{cond}(H_{fg} + c_{pv}T_{cond})] \qquad (1)$$

The total energy exchanged by the water flow over an incremental pipe surface (dA) can be expressed with convection coefficient between water and pipe surface h_{int},

$$dQ = h_{int} dA(T_{cond} - T_w) \qquad (2)$$

As in the analysis performed by Threlkeld (1970), it is possible to aggregate the two components' temperature and humidity differences in an equivalent enthalpy difference. For a Lewis value of unity (Sacadura 1993), considering the heat transfer coefficient, Equation (1) becomes

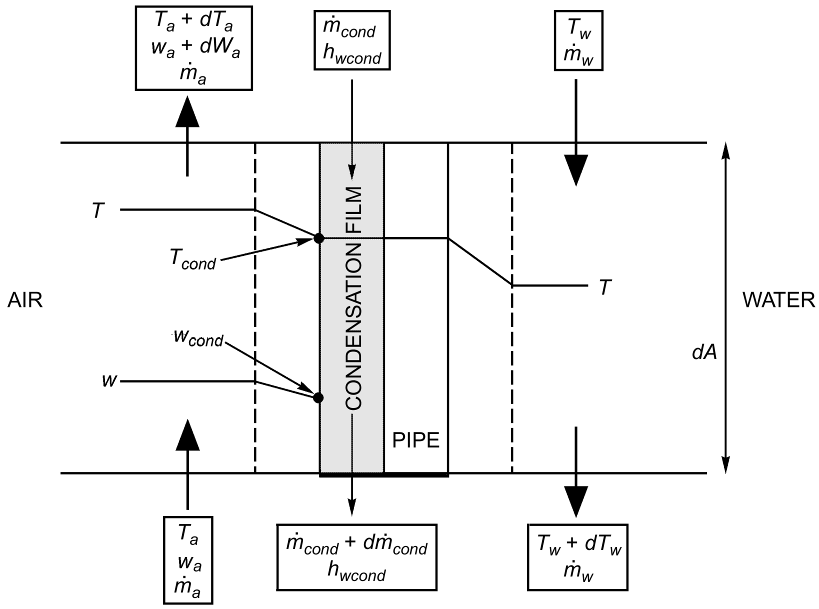

Figure 2. Heat and Mass Transfer in Cooling Coil

$$dQ = \frac{U_{ext}\,dA}{c_{pa}}(h_a - h_{condsat}) \tag{3}$$

In order to homogenize Equations (2) and (3), the air saturated enthalpy is assumed to be a linear function of temperature:

$$\Delta h_{sat} = c_{psat}\Delta T \tag{4}$$

Water is represented by the fictitious enthalpy of saturated air at water temperature, $h_{wsat}(T_w)$. The coefficient c_{psat} has the dimensions of heat capacity and is assumed to be constant for the considered range of temperature. Equation (2) becomes

$$dQ = \frac{U_{int}\,dA}{c_{psat}}[h_{condsat}(T_{cond}) - h_{wsat}(T_w)] \tag{5}$$

Using the fact that the exchanged energy rate is constant, the thermal resistance between air and water can be considered as an addition of resistances in series as shown in Figure 3. The equation of thermal and mass exchange is obtained by combining Equations (3) and (5):

$$dQ = U_h dA(h_a - h_{wsat}) \tag{6}$$

with

$$\frac{1}{U_d\,dA} = \frac{c_{pa}}{U_{ext}\,dA_{ext}} + \frac{c_{psat}}{U_{int}\,dA_{int}} \tag{7}$$

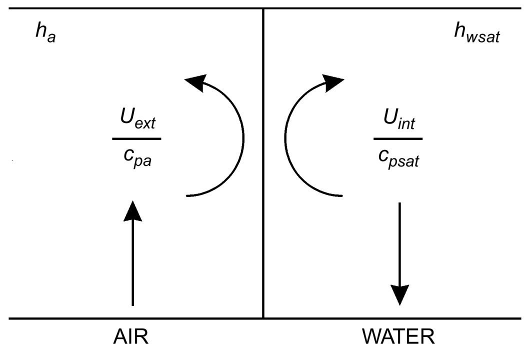

Figure 3. Heat and Mass Transfer in Cooling Coil: Representation Using Threlkeld (1970) Method

Two common techniques for thermal exchangers are applied to model heat and mass transfer for the cooling coil: the effectiveness method NTU-ε and the log mean temperature difference, ΔT_{lm}. Both methods can be used when condensation occurs by using air enthalpy instead of air temperature and fictitious saturated air enthalpy instead of water temperature (h_{wsat} instead of T_w). Both methods assume that the global exchange coefficient is constant for the heat and mass exchanger.

Cooling Coil Parameter Identification

The purpose of the parameter identification process is to characterize the cooling coil from available data. The most accurate approach for this process requires geometrical data, but in some applications users do not have geometrical data and do not have the time to collect it. That is the reason why CCDET model in ASHRAE *Toolkit* is rarely used by engineers for HVAC design. The nominal rating, which is generally available, is very often the only datum available to characterize the cooling coil.

As described previously, the internal and external heat exchange coefficients UA_{int} and UA_{ext} are characteristics of the cooling coil. They are respectively dependent on the water and airflow rates. The data used at this step are extracted from one nominal rating point of the cooling coil.

The common exchanger calculation techniques are applied to the cooling coil with heat and mass transfer described by Equation (6). The log mean enthalpy difference method is applied to the counterflow heat exchanger (which is a good assumption for crossflow with at least four rows).

$$Q_{rat} = UA_{hrat} \Delta h_{lmrat} \tag{8}$$

$$\Delta h_{lmrat} = \frac{(h_{ai} - h_{wosat}) - (h_{ao} - h_{wisat})}{\ln \dfrac{h_{ai} - h_{wosat}}{h_{ao} - h_{wisat}}} \tag{9}$$

Elmahdy and Mitalas (1977) demonstrated that a model based on this method has a maximal error of 4% compared to experimental data. This calculation method is advocated by ARI *Standard* 410 for forced-circulation air-cooling and air-heating coils.

The purpose is to obtain UA_h. To determine how UA_h varies with airflow and waterflow changes, estimate the internal and external heat transfer coefficients separately.

The airside heat exchange coefficient depends only on the airside coil geometry and on the airflow conditions. Thus, a fictitious coil can be considered to have equivalent conditions on the air side and infinite flow on the water side, as proposed in the simplified cooling coil model CCSIM of ASHRAE *HVAC 2 Toolkit* (Brandemuehl et al. 1993). The fictitious saturated air enthalpy of water, which is constant for the fictitious coil, is determined using inlet and outlet air condition. This enthalpy corresponds to apparatus dew-point temperature of the real coil. Then, the fictitious effectiveness of the cooling coil is calculated as follows:

$$\varepsilon_{fictitious} = \frac{h_{ai} - h_{as}}{h_{ai} - h_{adp}} \tag{10}$$

Considering the heat exchange resistance in Equation (7) and the NTU value in Equation (11), and assuming that the internal resistance is negligible compared to external resistance (infinite water flow rate), the UA_{ext} value is extracted from the effectiveness expression for coil with infinite water flow as shown in Equation (12). The minimal capacity rate C_{min} has the same unit as the overall enthalpy heat transfer coefficient. The relations are

$$\mathrm{NTU} = \frac{UA_{hrat}}{C_{min}} \tag{11}$$

$$\varepsilon_{fictitious} = 1 - e^{-\mathrm{NTU}} \tag{12}$$

$$UA_{exrat} = -\dot{m}_a c_{pa} \ln(1 - \varepsilon_{fictitious}) \tag{13}$$

The real value of the waterside heat transfer coefficient UA_{intrat} is extracted from the global and air-side coefficients using Equation (7). Using this approach, the characteristics of the cooling coil (heat transfer coefficients for air side and liquid side) are calculated for the nominal rating point. It is now necessary to evaluate those coefficients for nonnominal conditions.

Performance Calculation

Outlet air and water temperatures are calculated from inlet conditions and heat transfer coefficients using the NTU-ε method applied to heat and mass transfer between air and water (Dewitt and Incropera 1996).

In addition, it is necessary to determine whether the cooling coil is wet, dry, or partially wet. The calculations under wet or dry conditions are based on the Braun (1988) method, which shows that the performance of coils with partially wet surfaces can be approximated by assuming either fully dry or fully wet conditions, whichever predicts the maximal heat transfer rate. The assumption generally results in errors of less than 5% on total energy rate.

The approach of the simple model consists of calculating the impact of air and water mass flow rate variation on the heat exchange coefficient. It is then necessary to identify the correlation between the mass flow rates and the internal or external heat exchange coefficients. The detailed correlations are simplified. First, the water-side heat transfer coefficient is evaluated.

Assuming the pipe conductive resistance is negligible compared with the convective resistance, the internal heat transfer coefficient can be expressed as follows:

$$UA_{int} = A_{int} h_{int} \tag{14}$$

As the inside area is constant for one coil, the heat transfer coefficient varies with the convection coefficient. The Dittus-Boelter correlation (ASHRAE 1994) is used to determine the convection heat transfer coefficient h_{int} for a one-phase fluid from the Nusselt number and for Reynolds numbers larger than 2500:

$$\mathrm{Nu}_w = 0.023\mathrm{Re}_w^{0.8}\mathrm{Pr}_w^{0.4} \tag{15}$$

with

$$\mathrm{Nu}_w = \frac{d_{int}h_{int}}{\lambda_w},\ \mathrm{Re}_w = \frac{G_w d_{int}}{\mu_w},\ \mathrm{Pr}_w = \frac{\mu_w c_{pw}}{\lambda_w} \tag{16}$$

Thus,

$$UA_{int} = 0.023A_{int}\frac{\lambda_e}{d_{int}}\left(\frac{\dot{m}_w}{\pi d_{int}\mu_w}\right)^{0.8}\left(\frac{\mu_w c_{pw}}{\lambda_w}\right)^{0.4} \tag{17}$$

Rabehl et al. (1999) propose a method to fit coefficients or exponents of correlation. This method needs 16 performance values to fit correctly. Indeed, this technique allows extension to different heat transfer fluids, different temperature ranges and different temperature levels.

The model presented is applied only for a chilled water cooling coil. In the range of typical temperatures for air conditioning (typically 5 to 12°C), the water properties viscosity μ and thermal conductivity λ are assumed to be constant. Thus, for one coil (i.e., d_{int} and A_{int} are constant), the inside heat transfer coefficient depends only on water mass flow rate for turbulent flows. The nonrating value can be calculated from rating value by identifying all the constant (or assumed to be constant) values in Equation (17) using the known rating value as follows:

$$\frac{UA_{intrat}}{\dot{m}_{wrat}^{0.8}} = 0.023A_{int}\frac{\lambda_e}{d_{int}}\left(\frac{1}{\pi d_{int}\mu_w}\right)^{0.8}\left(\frac{\mu_w c_{pw}}{\lambda_w}\right)^{0.4} \tag{18}$$

which leads to

$$UA_{int} = \frac{UA_{intrat}}{\dot{m}_{wrat}^{0.8}}\dot{m}_w^{0.8} \tag{19}$$

Second, concerning the airside heat transfer coefficient determination for nonnominal conditions, the heat transfer coefficient is written using convection and fin resistances:

$$UA_{ext} = \frac{1}{R_{ext}} + \frac{1}{R_{ail}} \tag{20}$$

$$R_{ext} = \frac{1}{h_{ext}A_{ext}} \tag{21}$$

$$R_{ail} = \frac{1}{h_{ext}A_s\eta_{ail}} \tag{22}$$

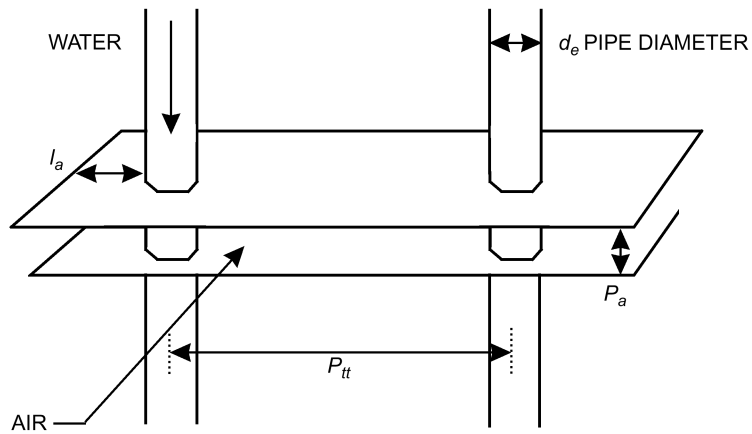

Figure 4. Fin and Pipe Configuration

First, the convection heat transfer coefficient for cooling coils with dry fin area is determined. This coefficient is calculated using the COLBURN factor j correlation presented in Equation (23) (Elmahdy and Mitalas 1977). The values of the geometrical parameters describing fins and pipes are explained in Figure 4.

$$h_{ext,dry} = jG_a c_{pa} \mathrm{Pr}_a^{-2/3} \tag{23}$$

$$j = c_1 \mathrm{Re}_a^{c_2} \qquad \mathrm{Re}_a = \frac{G_a d_h}{\mu_a} \qquad G_a = \rho_a v_a \frac{A_l}{A_a} \tag{24}$$

$$d_h = \frac{4A_a}{P} \qquad A_a = (P_a - e_a)(P_{tt} - d_e) \qquad P = 2(P_a - e_a) + 2(P_{tt} - d_e) \tag{25}$$

$$d_{ail} = \sqrt{\frac{4P_{tt}P_{lt}}{\pi}} \qquad l_a = 0.5(d_{ail} - d_e) \tag{26}$$

Where P_a is the fin spacing, P_{lt} is the row spacing, P_{tt} is the distance between tubes, d_e is the tube outside diameter, d_{ail} is the fin equivalent diameter and l_a is the fin equivalent height, as shown in Figure 4.

The c_1 and c_2 coefficients as determined by Elmahdy and Biggs (1979) from geometry data for $200 < \mathrm{Re}_a < 2000$ are as follows:

$$c_1 = 0.159\left(\frac{e_a}{1_a}\right)^{0.141}\left(\frac{d_h}{e_a}\right)^{0.065} \tag{27}$$

$$c_2 = -0.323\left(\frac{e_a}{1_a}\right)^{0.049}\left(\frac{P_a}{e_a}\right)^{0.077} \tag{28}$$

This chosen correlation has been compared with other correlations of literature:

Elmahdy and Biggs (1979)		
21 coils with flat fins and 4 to 8 rows j is obtained at ±10%	$j = c_1 \mathrm{Re}_{d_h}^{c_2}$ $c_1 = 0.159\left(\frac{e_a}{l_a}\right)^{0.141}\left(\frac{d_h}{e_a}\right)^{0.065}$	$200 < \mathrm{Re}_{d_h} < 2000$ $c_2 = -0.323\left(\frac{e_a}{l_a}\right)^{0.049}\left(\frac{P_a}{e_a}\right)^{0.077}$
Chuah et al. (1998)		
1 coil with flat fins and 3 rows and 3 rows test and correction of Elmahdy and Biggs (1979) on a specific coil	$j = c_1 \mathrm{Re}_{d_h}^{c_2}$ $c_1 = 0.101\left(\frac{e_a}{l_a}\right)^{0.141}\left(\frac{d_h}{e_a}\right)^{0.065}$	$200 < \mathrm{Re}_{d_h} < 2000$ $c_2 = -0.323\left(\frac{e_a}{l_a}\right)^{0.049}\left(\frac{P_a}{e_a}\right)^{0.077}$
Mirth and Ramadhyani (1993)		
5 coils with flat fins and 4 and 8 rows	$j = 0.13 \mathrm{Re}_{d_h}^{-0.33}$	$900 < \mathrm{Re}_{d_h} < 1700$
Wang, Fu, et al. (1997)		
18 coils with sinusoidal fins and 1 to 4 rows j is obtained at ±10%	$j = \frac{1.201}{[\ln(\mathrm{Re}_{d_e}^{\sigma})]}$ with $s = A_a/A_l$	$400 < \mathrm{Re}_{d_e} < 8000$
Wang, Hsieh, et al. (1997)		
9 coils with flat fins and 2 to 6 rows j is obtained at ±10%	$j = 0.4 \mathrm{Re}_{d_e}^{-0.468 + 0.0407N} \varepsilon^{0.159} N^{-1.261}$	$200 < \mathrm{Re}_{d_e} < 4000$
Turaga et al. (1988)		
10 coils with flat fins and 3 to 8 rows	$j = 0.053 \varepsilon^{-0.24} \mathrm{Re}_{d_h}^{-0.18}$	$300 < \mathrm{Re}_{d_h} < 1500$
McQuiston (1978)		
10 coils with flat fins and 4 rows j is obtained at ±10%	$j = 0.0014 + 0.2618(\mathrm{Re}_{d_e})^{-0.4}\left(\frac{4}{\pi}\frac{P_{lt}}{d_h}\frac{P_{tt}}{d_e}\sigma\right)^{-0.15}$ with $s = A_a/A_l$	

Results of the comparison are given in Figure 5. As the purpose is to express UA_{ext} from rating value UA_{ext}^{rat}, j/j_{nom} is plotted on Figure 5. All results are close except those of Turaga et al. (1988). The correlation of Wang, Fu et al. (1997) relative to coils with sinusoidal fins is in good agreement with the others; j_{nom} is larger but only j/j_{nom} is relevant.

Second, the fin efficiency is evaluated following Taborek et al. (1983) using the equivalent circular fin of diameter d_{ail}:

$$\eta_{ail} = \frac{\tanh(\alpha L)}{\alpha L} \tag{29}$$

$$\alpha = \sqrt{\frac{2h_{ext}}{\lambda_{ail} e_a}} \tag{30}$$

$$L = 0.5 d_e\left(\frac{d_{ail}}{d_e} - 1\right)\left[1 + 0.35 \ln\left(\frac{d_{ail}}{d_e}\right)\right] \tag{31}$$

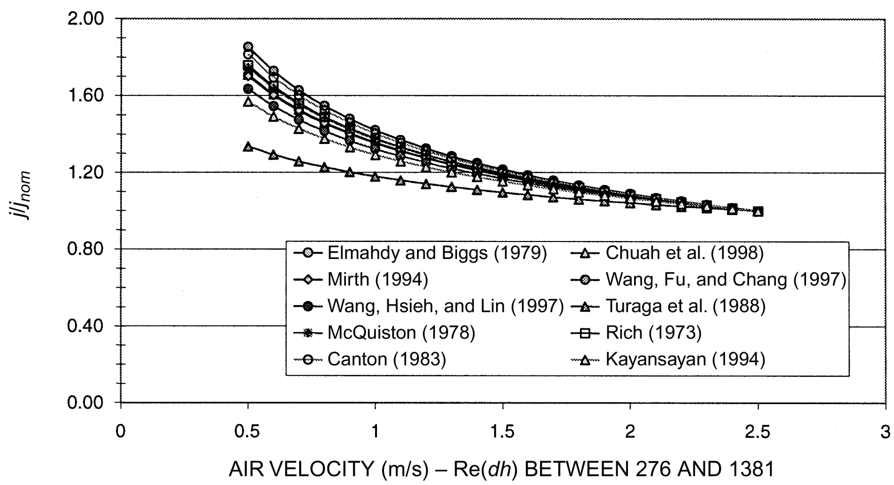

Figure 5. Comparison of Correlations for Air Side (Dry Conditions)

Third, the convection heat transfer coefficient for the cooling coil with wet fin area is determined. A corrective factor based on air velocity is introduced to take condensation into account (Threlkeld 1970):

$$h_{ext,wet} = C_f h_{ext,dry} \tag{32}$$

with C_f calculated from an experimental correlation considering 600 < Re < 2000,

$$C_f = 0.626(5.08 \times 10^{-3})^{0.101} v_f^{0.101} \tag{33}$$

where v_f is the air velocity in minimal section, $v_f = G_a/r_a$ m/s, with G_a mass flow rate per square metre.

All of these expressions require geometrical data that are often unknown at the HVAC design phase or that require too much time to be determined. It is necessary to determine UA_{ext} using a simplified approach. Experimental results suggest a correlation for h_{ext} expressed as

$$h_{ext} = aV_a^b \tag{34}$$

A survey of seven different cooling coil manufacturers' products shows that at the present time the cooling coil technology applied to building air conditioning is not significantly varied. Indeed, all manufacturers' products are similar: cooling coil with pipes and flat aluminum plate fins, as shown in Figure 1. Typically, the pipes are copper. Some coils have tube and fins of other material, but these coils are used in specific applications (operation with salt water, etc). The number of rows ranges from two to eight. For fewer than three rows, the assumption of counterflow exchanger is no longer valid, but this kind of cooling coil is not common. Fifty different cooling coil configurations have been found in manufacturers' catalogs (Table 1). For industrial applications, some coils can have different geometric characteristics such as a fin spacing of 15 mm, for example.

Table 1. Possible Existing Geometrical Configurations for Seven Cooling Coil Manufacturers

Coils Described	e_a, mm	$P_{tt} \times P_{lt}$, mm	P_a, mm	d_e, mm
Coil 1	0.12	30×30	1.6, 2, 2.5, 3	15.8 (5/8 in.)
		60×30	1.6, 2, 2.5, 3, 4	
Coil 2	0.12	30×30	Standard 2.2	
			Other available up to 4 mm	
Coil 3	0.12	25×25	Standard 2.5	9.5 (3/8 in.)
		30×30	1.6, 2, 2.5, 3.0, 4.0	(1/2 in.)
		60×30		15.8 (5/8 in.)
Coil 4	0.12	25×25	Standard 2.2	
		30×30		
Coil 5	0.18	30×30	2, 3, 4	(5/8 in.)
Coil 6	0.12	30×30	2.3, 2.5	9.5 (3/8 in.)
Coil 7	0.12	25×25	2.1	15.8 (5/8 in.)
		30×30		

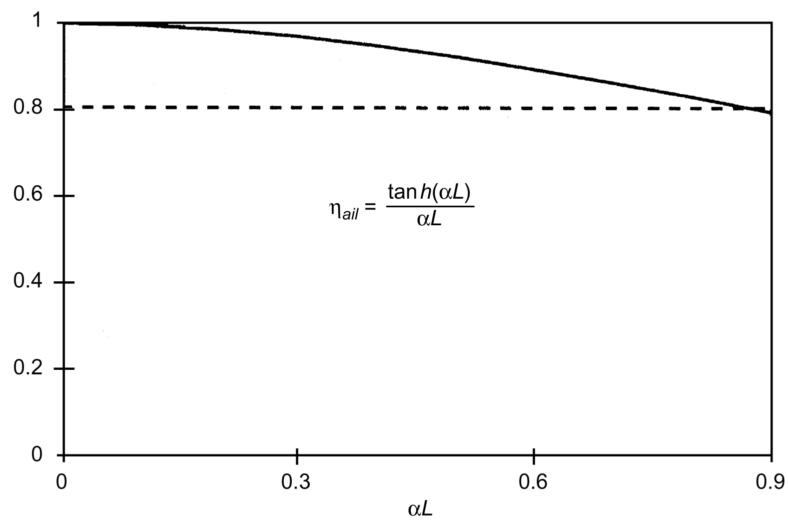

Figure 6. Typical Values of Fin Efficiency for Cooling Coil in Building

In the configurations presented, the maximal value for αL is considered. The extreme realistic values of parameters of Equations (30) and (31) are taken to be h_{ext} = 100 W/(m·K), λ_{ail} = 200 W/(m·K) (aluminum), e_a = 0.12 mm, and L = 10.1 mm.

The L value is calculated using a 30 by 60 mm configuration of 5/8 in. pipes, which is the existing configuration giving the highest L value. Those values give a maximum realistic value for αL of 0.9. Figure 6 shows that for the range of αL of 0 to 0.9 m^{-1}, the fin efficiency values vary from 1 to 0.8 and the slope of the variation is low. So, the fin efficiency can be considered as a constant. The narrow range of values of fin efficiency is due to the fact that the price of the fins is attributed to implementation, and that the cost of high-efficiency fins is actually low. So it is logical for the manufacturer to propose very efficient fins (more than 85%). With those assumptions, Equations (20) to (22) and (29) to (31) are simplified as indicated in Equation (35):

$$UA_{ext} = A_{cor} h_{ext} \tag{35}$$

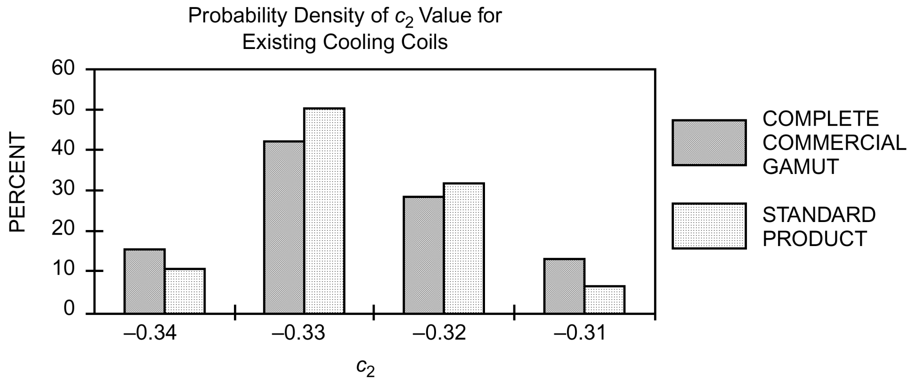

Figure 7. Statistic Distribution of c_2 Values for Range of Cooling Coils in Air-Conditioning Industry

Considering Equations (20) to (28) and a constant fin efficiency value, UA_{ext} varies only with the airflow rate. One should now determine the exponent b of the airflow rate as in Equation (34). It depends only on c_2 with the factor j provided by Equation (24) in the Reynolds number range [200 to 2000]. For all the 50 cooling coil configurations presented in Table 1, the c_2 coefficient is evaluated using Equation (28). The resulting distribution of the c_2 values is plotted in Figure 7 for the complete gamut of cooling coils. The variation range of c_2 value is –0.34 to –0.31. Thus, a default mean c_2 value can be defined:

$$c_2 = -0.33 \tag{36}$$

This default value corresponds to the following configuration, which is very common in building air-conditioning applications: P_{tt} = 30 mm, P_{lt} = 30 mm, P_a = 2.5 mm, e_a = 0.12 mm. Figure 7 depicts the distribution of c_2 weighed by the sales of each product. To have a more realistic distribution of the exponent c_2, the common coils (standard product) have been arbitrarily weighted by 0.8 and the unusual coils by 0.2. These values correspond to the fact that manufacturers produce about 80% of standard products and 20% of nonstandard products. About 50% of the most common cooling coils have a c_2 value of –0.33.

With this default value of c_2, the outside heat transfer in wet conditions UA_{ext} becomes

$$UA_{ext} = bv_a^{0.77} \tag{37}$$

Equation (37) is the condensed expression of Equations (20) to (33) according to the assumptions made. In dry conditions, the corrective factor C_f expressed in Equation (33) does not apply and the outside heat transfer UA_{ext} is then

$$UA_{ext} = bv_a^{0.67} \tag{38}$$

The experimental Nüsselt correlation determined by Mirth (1994) for the dry cooling coil agrees with the value obtained by this method in the case of dry regime.

$$\mathrm{Nu} = 0.13 - \mathrm{Re}^{0.67}\mathrm{Pr}^{1/3} \tag{39}$$

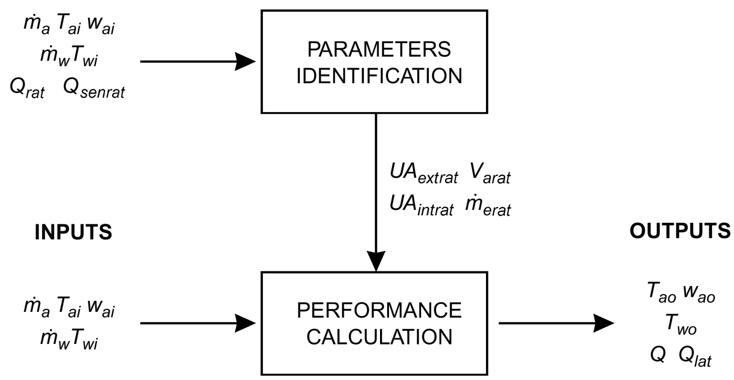

Figure 8. Architecture of Cooling Coil Model

The multiplier coefficient b in Equation (38) depends on thermal properties (viscosity, heat capacity, and conductivity) and on geometrical data. For typical cooling coil air temperature variation (15 to 30°C), the viscosity, heat capacity, and conductivity are assumed to be constant. Thus, b is identified for a rating point for a specific cooling coil and is a constant for this cooling coil. The volume airflow rate at inlet of the cooling coil is used instead of air velocity in order to reduce the cooling coil data needed.

$$UA_{ext} = \left(\frac{UA_{extrat}}{V_{arat}^{0.77}}\right)V_a^{0.77} \tag{40}$$

To make the calculations less complicated and to avoid an iterative process, the outside heat transfer correlation used for all cases (wet, dry, and partially wet) is Equation (40), which is specific for a wet regime. The effects of this assumption and of the default value for c_2 are discussed later.

The model architecture is illustrated in Figure 8. Both pairs of model characteristics (UA_{extrat}, V_{arat} and UA_{intrat}, $\dot{m}_{erat}$) are calculated from the nominal rating point values (i.e., $\dot{m}_a T_{ai} w_{ai}$ for air conditions, $\dot{m}_w T_{wi}$ for water conditions, and $Q_{rat} Q_{senrat}$ for outlet conditions). Then, using the characteristic values, the performance of the cooling coil is calculated from air and water inlet conditions for nonnominal operation.

SENSITIVITY TO ERRORS

The main assumptions of the model are integrated into the airside heat transfer correlation. For the UA_{ext} correlation, Mirth and Ramadhyani (1993) have shown that errors in experimental heat transfer rates are amplified when the convective heat exchange coefficient is determined. In contrast, the error is reduced when predicting heat transfer using a heat transfer coefficient correlation. Indeed, as demonstrated by Mirth and Ramadhyani (1993), a 20% uncertainty in the heat exchange coefficient results in an uncertainty of less than 5% in the predicted coil heat transfer rate. This effect is illustrated by the expression of the NTU-e relation for a counterflow exchanger considering the range of NTU values.

The effects on the calculated energy rate of the main assumptions made are determined first using various methods, including the statistical Monte Carlo method. Second, the estimation of the uncertainty induced from characterization data is evaluated.

As described in Aude et al. (1997), a probability density is assigned to all the uncertain inputs of the model. For each simulation, one value is selected randomly for each input based on its probability of occurrence. Assuming the inputs are normally distributed, the extreme values are less likely to be selected that the central value. Because all the inputs are perturbed simultaneously, this method fully accounts for any interactions between the inputs. The process is repeated many times and, after several simulations, the standard deviation of each output of the model can be estimated. The accuracy of the standard deviation estimation depends only on the number of simulations.

All the uncertain parameters (T_{ai}, w_{ai}, $\dot{m}_a$, T_{wi}, and $\dot{m}_w$) are simultaneously perturbed. For each set of random input data, the simulation is carried out. For instance, standard deviation σ_{Tao} on output air temperature T_{ao} is shown in Figure 9. This standard deviation depends on the number of simulations carried out. Figure 9 shows σ_{Tao} as a function of the number of simulations for 10% uncertainty on cooling coil input data (see Table 2). The standard deviation s_{Tao} first varies between maximum and minimum values, then converges as the number of simulations increases. At 5000 simulations, convergence is reached; therefore, the following sensitivity analysis is carried out to 5000 simulations. The uncertainty on the standard deviation of the outputs is 15% for 100 simulations, 4% for 750 simulations, and 1% for 5000 simulations. This method is easy to use and well adapted for complex models for which analytical methods of uncertainty prediction are not applicable, but requires long computer time.

The main assumption of the model is the air-side heat transfer correlation, and particularly on the default value for c_2. Using the statistic distribution of the parameter c_2 for the complete commercial gamut as presented in Figure 7, the probability density of c_2 is evaluated for the 5000 simulations. The Monte Carlo method is applied with this probability density as an input for the parameter c_2 value. The nominal rating point used to determine the parameters of the cooling

Table 2. Uncertainty on Input Data

Variables	T_{ai}	w_{ai}	$\dot{m}_a$	T_{wi}	$\dot{m}_w$
Units	°C	kg/kg	kg/s	°C	kg/s
Values	23.1	0.01118	0.6	9	0.4
Absolute/relative uncertainty	2.3°C	10%	10%	0.9°C	10%

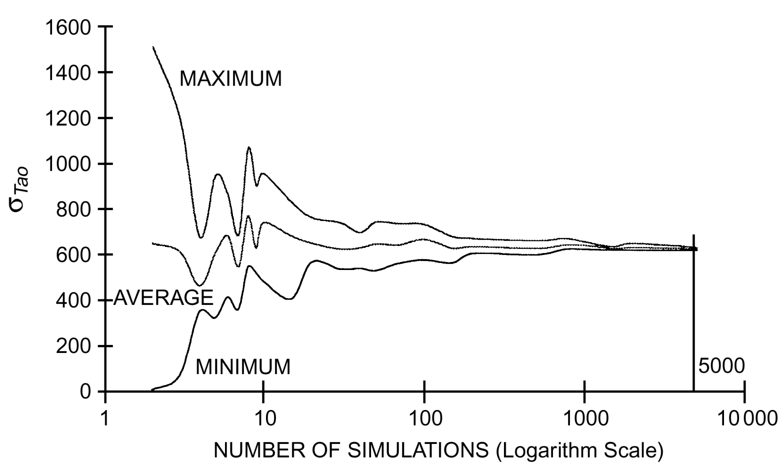

Figure 9. Evolution of Standard Deviation σ_{Tao} According to Number of Simulations in Monte Carlo Method

Table 3. Nominal Rating Point

Inputs	$\dot{m}_a$	T_{ai}	w_{ai}	$\dot{m}_w$	T_{wi}	Q	Q_{sen}	UA_{extrat}	V_{arat}	UA_{intrat}	$\dot{m}_{wrat}$
Units	kg/s	°C	kg/kg	kg/s	°C	W	W	W/K	m^3/s	W/K	kg/s
Rating point	0.85	23.1	0.01118	0.636	9	8508	6499				
Operation point	0.3	28	0.013	0.3	6			1633	0.726	2427	0.636

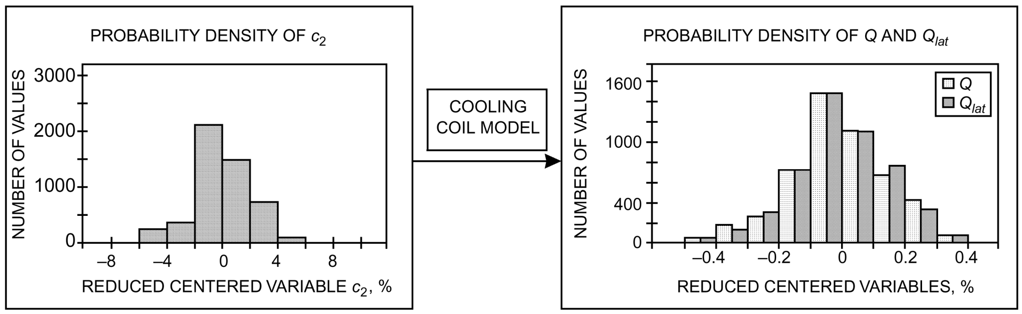

Figure 10. Impact of c_2 Assumption on Energy Rate Uncertainties

coil and the operation point applied to the cooling coil for the simulation are presented in the Table 3. The operation point, and particularly the airflow rate, is largely different from the nominal rating point in order to magnify the induced error on the UA_{ext} calculation.

The relative uncertainty calculated using a normal law hypothesis for the c_2 distribution is 3%. The order of magnitude for the relative uncertainties for the outlet conditions and total and latent energy rates is roughly 0.2%. The probability densities of the two energy rates are presented in Figure 10. Notice that the reduced centered variable is introduced as follows:

$$X_{red\ cent} = \frac{X - \overline{X}}{\overline{X}} \tag{41}$$

The uncertainty prediction calculation shows that the default value for the c_2 parameter induces a minor uncertainty on the outputs of the cooling coil model and produces a very small effect on the energy rate calculation.

In order to reduce the complexity of the calculation, the outside correlation UA_{ext} used for the calculation assumes the coil completely wet. This assumption does not mean the model always considers condensation. The deviation introduced by this method is the difference between the calculation made with a wet UA_{ext} value compared to a dry value for a cooling coil operating under dry conditions. The deviation on UA_{ext} is presented in Figure 11 for different values of inlet conditions, airflow rate, and water flow rate. The deviation on UA_{ext} implies a deviation on the result of total energy rate about four times smaller. The uncertainties on total energy rate introduced by the use of wet correlation for all cases are always lower than 3%. Using the wet correlation agrees with the accuracy required by the global method and prevents time-expensive iterations that are not desirable if the model is to be integrated in building simulation program.

To evaluate the error induced by the wet or dry determination method, the detailed model of ASHRAE *Toolkit* is used as a reference model. Indeed, this model calculates the heat transfer coefficient on the air and water sides from geometric coil data and from flow characteristics. The proportion of wet surface is calculated using the iterative method in the case of a partially wet regime. The model is applied to a typical 9000 m^3/h air handler cooling coil. The coil has

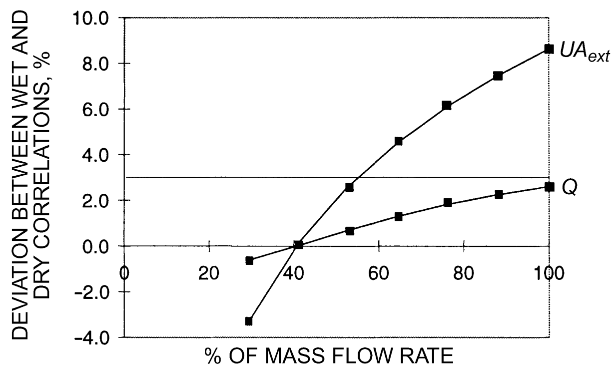

Figure 11. Deviation Caused by Use of Wet Correlation in Dry Conditions

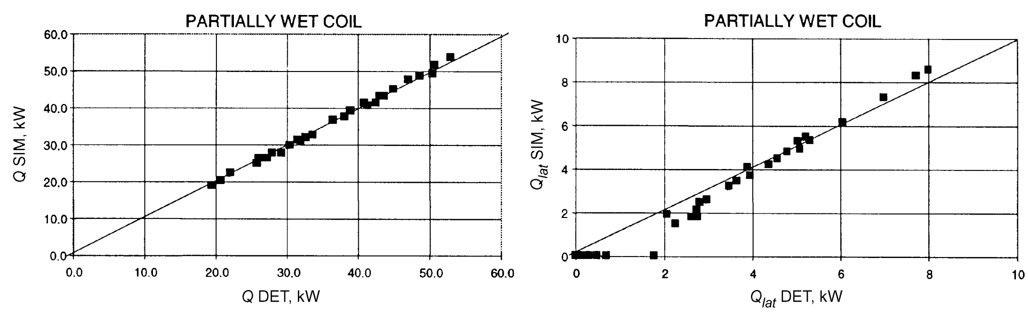

Figure 12. Difference Between Detailed and Simplified Model for Energy Rate and Latent Energy Rate: Cooling Coil Under Partially Wet Conditions

smooth copper tubes (15.3 mm ID for 1 mm of thickness) with flat aluminum plate fins. The coil is 4 rows deep and 22 tubes high, with 25 mm tube spacing. Moreover, the coil has a face area of 2.2 m^2, with an external heat transfer surface of 178.6 m^2 and internal heat transfer area of 11.3 m^2. The fins are 0.19 mm thick and the fin diameter is 38 mm. There are 288.714 fins per metre. Calculations are made for an airflow variation from 30% to 100% of its rating value (1) for a cooling coil using a water temperature control device (5 to 7°C) and (2) using a flow regulation device (25 to 100%). Entering air and humidity conditions of moist air vary from 24°C and 8 g/kg to 30°C and 10 g/kg. The results of the calculation of the energy rates are presented in Figures 12 and 13 for a partially wet cooling coil. The average relative difference observed is 1.5% on total energy rate, with a maximum relative difference of 4.7%.

For the latent energy rate due to condensation, there are two main cases, attributed to the method used to perform the calculation:

- For a condensation energy rate less than 2 kW (corresponding to 20% of the nominal value of latent energy rate), the simplified model considers the coil to be completely dry and considers the exchanged latent energy rate as the sensible energy rate. As a consequence, the overestimation on the sensible energy rate is 1.7% on average, with a maximum of 4.3%.
- For condensation energy rates over 2 kW, the simplified model considers the cooling coil to be completely wet. Between 2 kW and approximately 5 kW, the latent energy rate is underestimated. The mean difference is 14% and the maximum difference is 35%. For values over 5 kW, the latent energy rate is overestimated. The average difference is 5% and the maximum difference is 9%.

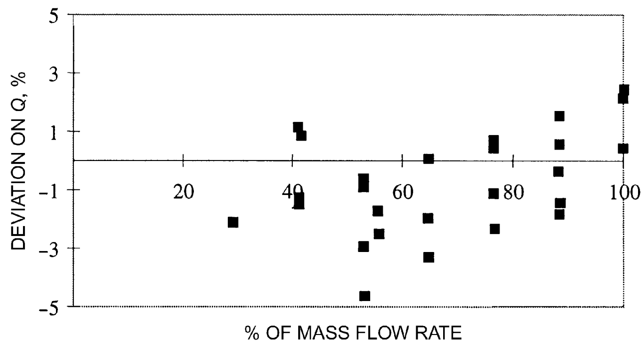

Figure 13. Deviation Between Simplified and Detailed Models for Partially Wet Conditions, %

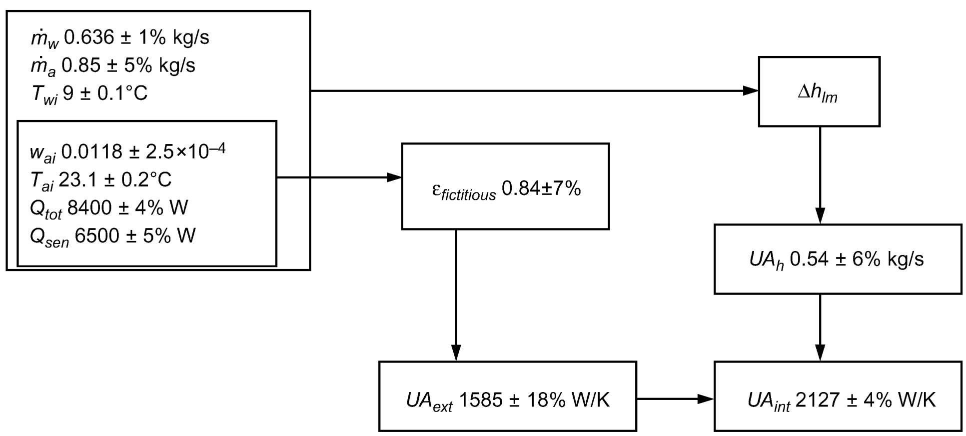

Figure 14. Errors Introduced by Data Characterization: Parameter Identification

Thus, the difference of the energy rate required from the chilled water is 1.5% on average, corresponding to the difference in the total energy rate. On the other hand, the difference in ambient conditions (indoor temperature and humidity) is more important due to the difference in distribution between the sensible and latent energy rates. The maximum difference in outlet air temperature is 24% and on outlet humidity is 13%. The average difference for both temperature and humidity under partially wet regime is less than 2%.

In the global HVAC system consumption estimation, the error introduced by the hypothesis on the partially wet regime is reduced. Indeed, if the model for a time step underestimates dehumidification, an artificial increase of the indoor humidity will be induced. So, at the next step, since the air will be more humid, the model will overestimate the dehumidification and will partially compensate for the error of the previous step.

After validating the main assumptions of the model, the next step is to determine the uncertainties induced by the use of nominal rating point values and the associated uncertainties. The nominal rating point includes seven variables. The uncertainty of each variable is given by the French Standard for fan coils (NF *Standard* E 38). The values, which are similar to American standard value for testing cooling coils, are summarized in Figure 14. Some uncertainties are expressed in percentage and others in absolute values. It is necessary that only independent variables should be used to introduce uncertainties.

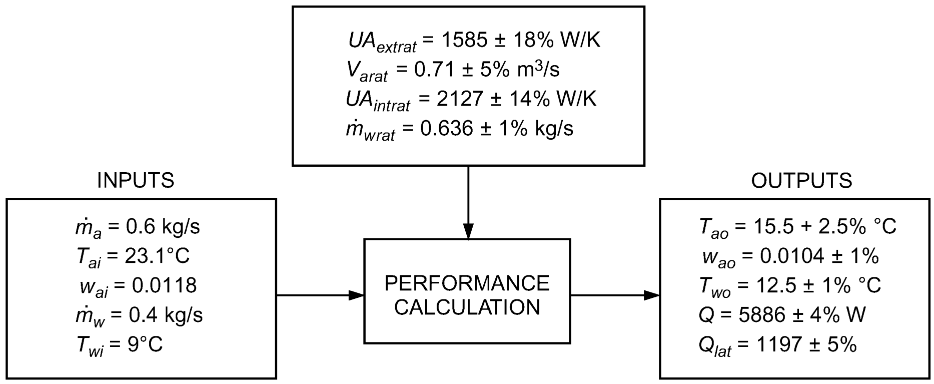

Figure 15. Errors Introduced by Data Characterization: Performance Calculation

Normal laws are considered for all input variables to determine the air and water exchange coefficients linked to the associated flow rate. The probability density of the output agrees with the assumption of normal laws. The uncertainties calculated during the parameter identification process are summarized in Figure 14. This figure shows that uncertainties are important when calculating air-side exchange coefficient from a fictitious effectiveness using Equation (13), which results from the use of the logarithmic function for a value near zero.

The Monte Carlo method is applied to consider the calculated density probability for the parameters and constant values for the inputs that are different from the rating point. The method and values used to study the error propagation and the uncertainties of the outputs of the model are summarized in Figure 15. The results indicate that the method using a nominal rating point is accurate, provided that the measurements at rating point meet the requirements for standard precision. Indeed, the use of the NTU-ε expression reduces the uncertainties caused by outside exchange coefficient.

EXPERIMENTAL VALIDATION OF THE MODEL

The experimental setup used to validate the model is presented in Figure 16. The setup consists of a variable air volume system. The air was circulated by two variable-speed centrifugal fans (1500 to 4500 m^3/h), one for supply air and one for exhaust air. The coil was controlled with a temperature-control device. Particular attention was devoted to measurement of airflow rate. The supply airflow rate was measured with a hot-wire anemometer at four places in the circular duct. The calculated error of the airflow rate measurement is 3%, including error of the method and error of the sensors. The water flow rate uncertainty is 0.05 m^3/s. Uncertainties are 0.2°C for air and water temperature measurements, and the relative uncertainty is 1.5% for absolute air humidity. The experiments are made for an airflow variation from 30 to 100% of its rating value for the cooling coil using a water temperature control device (7 to 12°C). Inlet air temperature and humidity conditions vary from 17°C and 45 g/kg to 24°C and 72 g/kg. The nominal rating point used to characterize the model is taken from measurement. Input data are represented on Figure 17 and details are given in the Appendix.

The coil is equipped with sinusoidal fins. Its characteristics are presented in Table 4. The calculations of uncertainties are carried out for the measurements using the Monte Carlo method. This leads to a ±200 W (5%) error on total energy rate and ±130 W (9%) error on latent energy rate. It should be noted that, in this case, latent energy rate is not calculated from condensation flow rate, which was not measured, but from outlet air conditions. Figures 18 and 19 present the results of the comparison for energy rate and temperature. Concerning total energy rate, the

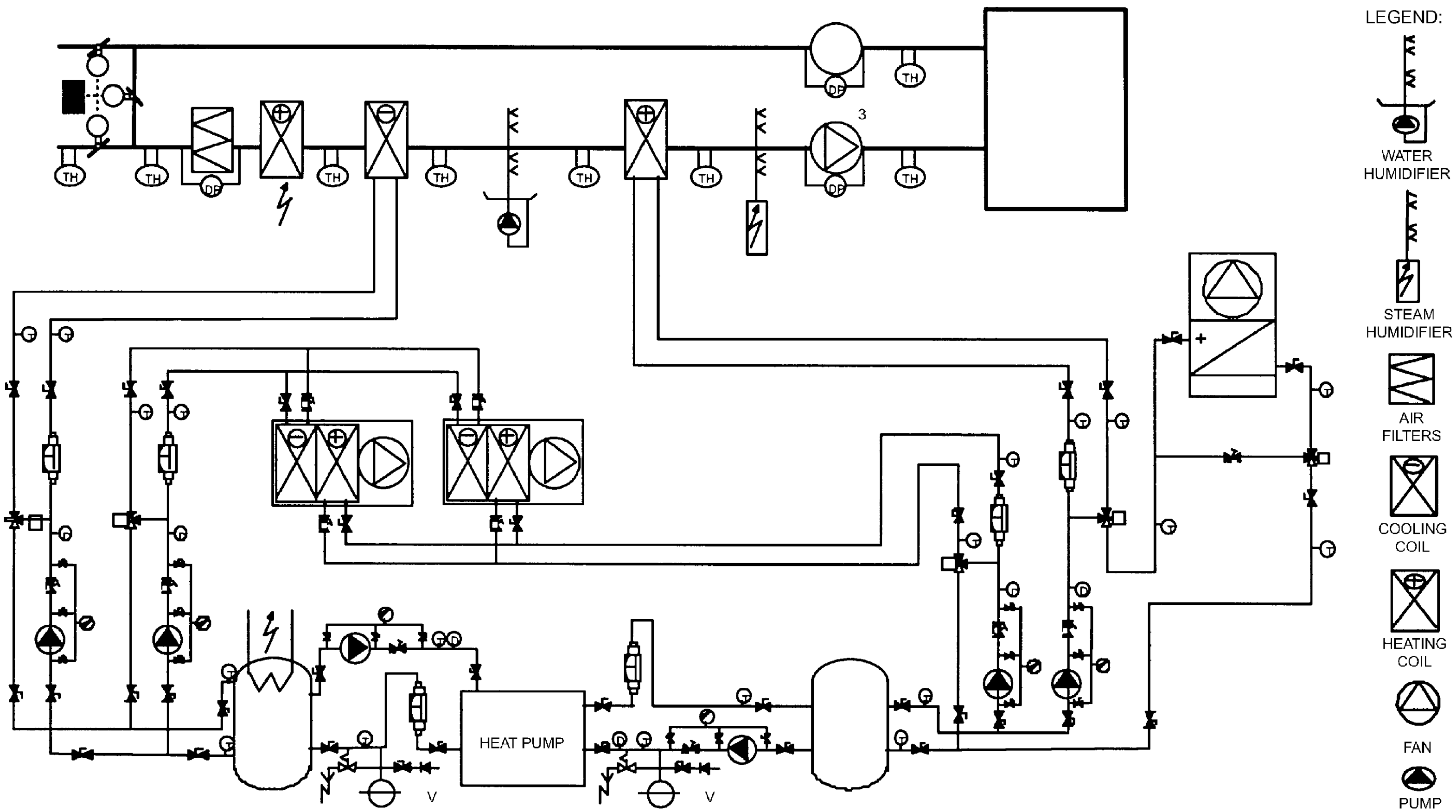

Figure 16. Experimental Apparatus

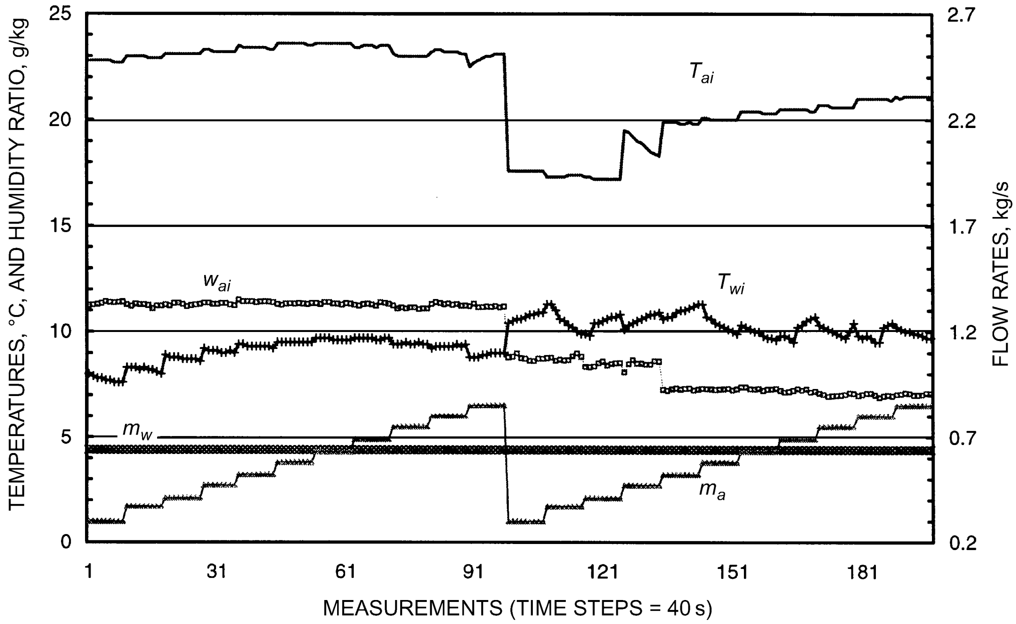

Figure 17. Experimental Input Data

Table 4. Coil Characteristics

Number of rows	4
Number of circuits	22
Duct height parallel to the tubes, m	0.61
Duct width, m	0.638
Outside tube diameter, m	0.0127
Inside tube diameter, m	0.0109
Thermal conductivity of tube material, W/(m·K)	389
Thickness of individual fin, m	0.0002
Spacing between individual fins, m	0.0018
Number of fins	305
Thermal conductuivity of fins, W/(m·K)	200
Distance between centers of tubes in a row, m	0.029
Distance between centerlines of tube rows, m	0.026
Specific heat of water + 20% ethylene glycol, J/(kg·K)	3800

calculated value fits into the measured value with a mean absolute relative error of 3%, including wet and partially wet operation. The absolute error on energy rate is in the range of value of the uncertainties on measured energy rate (±200 W). Moreover, the outlet air temperature given by the model agrees with the measured temperature with a mean absolute error of 0.3°C, with a maximal and minimal error of respectively 1°C and –0.5°C. Concerning the latent energy rate, (1) operation under wet conditions (1.8 to 2.45 kW) is well represented by the model and introduces a mean relative error of 3%; and (2) during operation under partially dry and wet conditions (0 to 0.7 kW), the latent energy rate is underestimated because of the method used to perform the calculation. This phenomenon occurs for low values of latent energy rate, and the induced error has a minimal influence on the building energy consumption estimation, as explained previously.

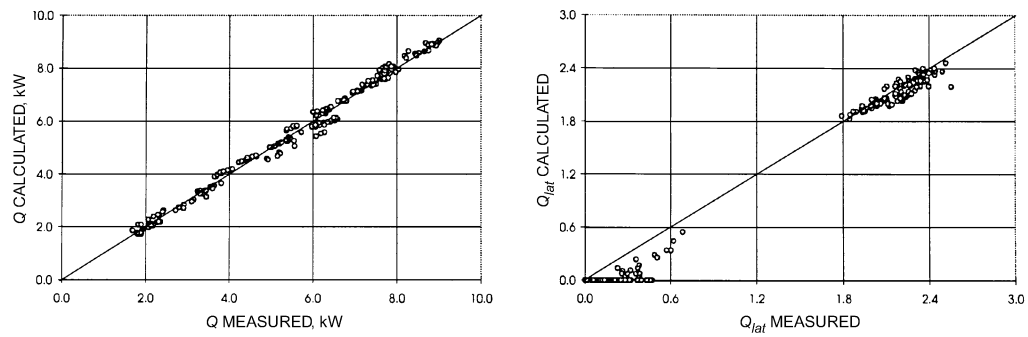

Figure 18. Experimental Validation on Energy Rate and Latent Energy Rate

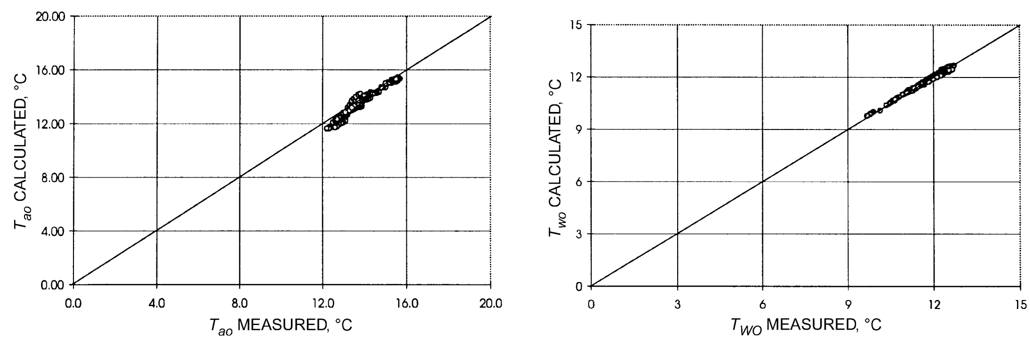

Figure 19. Experimental Validation on Outlet Air Temperature and Outlet Water Temperature

The experimental validation demonstrates the accuracy of the model and sheds light on the precautions that should be taken for a good use of the model. The model is well adapted to the global building energy consumption. Other applications of the model are feasible, after allowing for the relative inaccuracy in modeling partially wet regimes.

CONCLUSION

The proposed method for modeling cooling coils can be easily integrated into methods for estimating the energy use in buildings. The three main advantages of the model are

- Detailed cooling coil geometrical data are not required; only one nominal rating point is used to characterize the coil.
- The model is accurate under nonnominal conditions.
- The noncontrolled dehumidification energy rate is estimated correctly.

Therefore, this model allows the real operating performance of the cooling coil to be taken into account without significant computational efforts. This model has been integrated in the ConsoClim method (Morisot et al. 1997) for estimating building energy consumption.

NOMENCLATURE

A	air-side exchange area, m^2
A_{int}	water-side exchange area, m^2
A_l	airflow maximal area, m^2
A_a	airflow area, m^2
A_s	airflow fin area, m^2
A_{cor}	air-side exchange area corrected by fin efficiency, m^2
c_{pa}	specific heat of air, J/(kg·K)

c_{psat} specific heat of saturated air, J/(kg·K)
c_{pw} specific heat of liquid water, J/(kg·K)
c_{pv} specific heat of water vapor, J/(kg·K)
c_1, c_2 coefficient for *j* factor from COLBURN correlation
C_{min} minimal capacity rate between air and water, kg/s
d_{int} inside pipe diameter, m
$d_{h,}$ air-side hydraulic diameter, m
d_e outside tube diameter, m
d_{ail} equivalent circular fin diameter, m
e_a fin thickness, m
h_{adp} enthalpy of saturated air at apparatus dew-point temperature, J/kg
h_{ext} convection heat transfer coefficient on air-side, W/(m^2·K)
h_{extwet} convection heat transfer coefficient for wet coil, W/(m^2·K)
h_{extdry} convection heat transfer coefficient for dry coil, W/(m^2·K)
h_{int} convection heat transfer coefficient on liquid-side, W/(m^2·K)
h_{mas} mass transfer coefficient, kg/(m^2·s)
h_a enthalpy of air, J/kg
h_{wsat} enthalpy of saturated air at liquid temperature, J/kg
H_{fg} heat of vaporization at 0°C, J/kg
G_a mass flux (flow/area), kg/(m^2·s)
j factor of COLBURN correlation
l_a equivalent fin height, m
$\dot{m}_a$ mass air flow rate, kg/s
$\dot{m}_w$ mass water flow rate, kg/s
$\dot{m}_{cond}$ condensation flow rate, kg/s
N number of rows of the coil
R_{ail} fin thermal resistance, K/W
R_{ext} fin air-side convection resistance, K/W
Nu Nusselt number
NTU number of transfer unit
P_a fin spacing, m
Pr Prandtl number
P_{tt} transverse tube spacing, m
P_{lt} longitudinal tube spacing, m
Q total energy rate, W
Re Reynolds number
T temperature, K
UA_h overall enthalpy heat transfer coefficient, W/K
UA_{ext} air-side heat transfer coefficient, W/K
UA_{int} liquid-side heat transfer coefficient, W/K
v_a front face velocity, m/s
v_w front water velocity, m/s
V_a specific dry air volumetric flow rate, m^3/s
w humidity ratio, kg/kg dry air
X variable
$\bar{X}$ average value of the population of X variable
Δh_{lm} log mean enthalpy difference, J/kg
α constant
ε coil effectiveness or fin factor
$\varepsilon_{fictitious}$ coil effectiveness of fictitious coil with infinite water flow rate
η_{ail} fin efficiency
λ_a thermal air conductivity, W/(m·K)
λ_w thermal water conductivity, W/(m·K)
μ_a dynamic air viscosity, Pa/s
μ_w dynamic water viscosity, Pa/s
ν_a kinematic air viscosity, m^2/s
ρ_a air density, kg/m^3
ρ_w water density, kg/m^3

Subscripts

i inlet
o outlet
a air
w water
cond condensation film
rat related to the nominal rating point
sat at saturation

REFERENCES

ARI. 1987. *Forced-Circulation Air-Cooling and Air-Heating Coils*. ARI S*tandard* 410-87. Arlington, Virginia: Air-Conditioning and Refrigeration Institute.

ASHRAE. 1994. 1994 *ASHRAE Handbook—Fundamentals*. Atlanta: American Society of Heating, Refrigerating and Air-Conditioning Engineers.

Aude, P., P. Depecker, and J. Virgone. 1997. Building Thermal Modelling: An Example of Radiative Exchange Between System and Envelope Taking Account Uncertainties. *Clima2000 Proceedings*, Brussels, CD-ROM.

Brandemuehl, M.J., S. Gabel, and I. Andersen. 1993. *A Toolkit for Secondary HVAC System Energy Calculations*. Published for ASHRAE by Joint Center for Energy Management, University of Colorado at Boulder.

Braun, J.E. 1988. *Methodologies for the Design and Control of Central Cooling Plants*. Ph.D. dissertation, University of Wisconsin, Madison.

Chuah, Y.K., C.C. Hung, and P.C. Tseng. 1998. Experiments on the Dehumidification Performance of a Finned Tube Heat Exchanger. *International Journal of HVAC & Research* 4(2):167-178.

Dewitt, D.P. and F.P. Incropera. 1996. *Fundamentals of Heat and Mass Transfer*, 4th ed. New York: John Wiley.

Elmahdy, A.H. and R.C. Biggs. 1979. Finned Tube Heat Exchanger: Correlation of Dry Surface Heat Transfer Data. *ASHRAE Transactions* 85(2).

Elmahdy, A.H., and G.P. Mitalas. 1977. A Simple Model for Cooling and Dehumidifying Coil for Use in Calculating Energy Requirements for Buildings. *ASHRAE Transactions* 83(2):103-117.

Holmes, M.J. 1988. *IEA Annex 10: System Simulation—Heating and Cooling Coils*. Arup Research and Development, U.K.

McQuiston, F.C. 1978. Correlation of Heat and Mass and Momentum Transport Coefficients for Plate-Finned Tube Heat Transfer Surfaces with Staggered Tubes. *ASHRAE Transactions* 84(1):294-309.

Mirth, D.R. 1994. *Experimental Studies and Mathematical Modeling of Chilled-Water Cooling Coils*. Ph.D. dissertation, Purdue University, West Lafayette, Indiana.

Mirth, D.R. and S. Ramadhyani. 1993. Prediction of Cooling Coil Performance Under Condensing Conditions. *International Journal of Heat and Fluid Flow* 14 (4):391-400.

Morisot, O. 2000. *Modèle de batterie froide à eau glacée adapté à la maitrise des consommations d'énergie.* Thèse de doctorat, Ecole des Mines de Paris.

Morisot, O., J.R. Millet, and D. Marchio. 1997. Simple Modeling for Energy Consumption Estimation in Air Conditioned Buildings. *Clima2000 Proceedings*, Brussels, CD-ROM.

NF. 1994. Echangeurs thermiques, Ventilo-convecteurs à eau. NF *Standard* E 38-332. ISSN 0335-3931, December.

Rabehl, R.J., J.W. Mitchell, W.A. Beckman. 1999. Parameter Estimation and the Use of Catalog Data in Modeling Heat Exchangers and Coils. *International Journal of HVAC & Research* 5(1):3-17.

Sacadura, J.F. 1993. *Initiation aux Transferts Thermiques*. 4th edition. Paris: Tec et Doc Lavoisier.

Taborek, J., G.F Hewitt, and N. Afgan. 1983. *Heat Exchangers: Theory and Practice*. New York: Hemisphere.

Threlkeld, J.L. 1970. *Thermal Environmental Engineering*, 2nd ed. Englewood Cliffs, New Jersey: Prentice-Hall.

Turaga, M, S. Lin, and P.P. Fazio. 1988. Correlations for Heat Transfer and Pressure Drop Factors for Direct Expansion Air Cooling and Dehumidifying Coils. *ASHRAE Transactions* 94(2):616-630.

Wang, C.C, Y.C. Hsieh, and Y.T. Lin. 1997. Performance of Plate Finned Tube Heat Exchanger Under Dehumidifying Conditions. *Journal of Heat Transfer* 119:109-117.

Wang, C.C., W.L. Fu, and C.T. Chang. 1997. Heat Transfer and Friction Characteristics of Typical Wavy Fin-and-Tube Heat Exchanger. *Experimental Thermal and Fluid Science* 14:176-186.

Appendix: Experimental Data

T_{ao}, °C	w_{ao}, g/kg da	T_{wo}, °C	$\dot{m}_w$, kg/s	T_{ai}, °C	w_{ai}, g/kg da	$\dot{m}_a$, kg/s	T_{wi}, °C	T_{ao}, °C	w_{ao}, g/kg da	T_{wo}, °C	$\dot{m}_w$, kg/s	T_{ai}, °C	w_{ai}, g/kg da	$\dot{m}_a$, kg/s	T_{wi}, °C
11.3	8.33	10.3	0.639	22.8	11.2	0.30	8.0	11.4	8.36	11.4	0.639	17.6	8.8	0.30	10.5
11.3	8.31	10.3	0.639	22.8	11.3	0.30	7.9	11.5	8.43	11.5	0.639	17.6	9.0	0.30	10.6
11.2	8.29	10.2	0.639	22.8	11.3	0.30	7.8	11.4	8.38	11.5	0.639	17.6	8.7	0.30	10.6
11.2	8.3	10.2	0.639	22.8	11.3	0.30	7.8	11.5	8.42	11.6	0.639	17.6	8.7	0.30	10.7
11.2	8.29	10.1	0.639	22.8	11.4	0.30	7.7	11.5	8.43	11.6	0.639	17.6	8.6	0.30	10.8
11.2	8.29	10.1	0.639	22.8	11.4	0.30	7.7	11.5	8.43	11.6	0.639	17.6	8.6	0.30	10.8
11.2	8.25	10	0.639	22.7	11.4	0.30	7.6	11.6	8.49	11.7	0.639	17.6	8.7	0.30	10.9
11.2	8.26	10	0.639	22.7	11.4	0.30	7.6	11.6	8.49	11.7	0.639	17.6	8.7	0.30	10.9
11.2	8.26	10	0.639	22.7	11.4	0.30	7.6	12	8.68	12.1	0.639	17.3	8.7	0.37	11.3
12.2	8.85	10.9	0.639	23	11.3	0.37	8.3	12	8.69	12.1	0.639	17.3	8.8	0.37	11.3
12.2	8.84	10.9	0.639	23	11.2	0.37	8.3	11.8	8.54	11.9	0.639	17.3	8.6	0.37	11.0
12.2	8.86	10.9	0.639	23	11.3	0.37	8.3	11.6	8.46	11.6	0.639	17.3	8.7	0.37	10.6
12.2	8.83	10.8	0.639	23	11.3	0.37	8.2	11.5	8.42	11.5	0.639	17.3	8.6	0.37	10.5

Appendix: Experimental Data (*Continued*)

T_{ao}, °C	w_{ao}, g/kg da	T_{wo}, °C	$\dot{m}_w$, kg/s	T_{ai}, °C	w_{ai}, g/kg da	$\dot{m}_a$, kg/s	T_{wi}, °C	T_{ao}, °C	w_{ao}, g/kg da	T_{wo}, °C	$\dot{m}_w$, kg/s	T_{ai}, °C	w_{ai}, g/kg da	$\dot{m}_a$, kg/s	T_{wi}, °C
12.2	8.85	10.9	0.639	23	11.3	0.37	8.3	11.4	8.37	11.3	0.639	17.4	8.7	0.37	10.3
12.1	8.82	10.8	0.639	22.9	11.2	0.37	8.2	11.4	8.4	11.3	0.639	17.4	8.8	0.37	10.2
12.1	8.78	10.8	0.639	22.9	11.1	0.37	8.2	11.4	8.37	11.2	0.639	17.4	9.0	0.37	10.0
12.1	8.79	10.7	0.639	22.9	11.2	0.37	8.1	11.2	8.3	11.1	0.639	17.4	8.8	0.37	9.9
12.1	8.77	10.6	0.639	22.9	11.2	0.37	8.0	11.2	8.18	11	0.639	17.3	8.3	0.41	9.9
12.8	9.19	11.6	0.639	23.1	11.3	0.41	8.9	11.1	8.14	10.9	0.639	17.3	8.3	0.41	9.8
12.7	9.15	11.5	0.639	23.1	11.2	0.41	8.8	11.4	8.28	11.4	0.639	17.2	8.3	0.41	10.4
12.8	9.19	11.5	0.639	23.1	11.3	0.41	8.8	11.5	8.37	11.4	0.639	17.2	8.5	0.41	10.4
12.8	9.19	11.5	0.639	23.1	11.4	0.41	8.8	11.6	8.43	11.5	0.639	17.2	8.6	0.41	10.5
12.7	9.15	11.4	0.639	23.1	11.3	0.41	8.7	11.6	8.36	11.6	0.639	17.2	8.4	0.41	10.6
12.7	9.12	11.4	0.639	23.1	11.2	0.41	8.7	11.6	8.41	11.7	0.639	17.2	8.5	0.41	10.7
12.7	9.14	11.4	0.639	23.1	11.2	0.41	8.7	11.7	8.44	11.7	0.639	17.2	8.5	0.41	10.7
12.7	9.15	11.4	0.639	23.1	11.3	0.41	8.7	11.7	8.46	11.8	0.639	17.2	8.5	0.41	10.8
12.7	9.13	11.3	0.639	23.1	11.3	0.41	8.6	11.8	8.08	11.6	0.639	19.5	8.1	0.47	10.1
13.4	9.55	12	0.639	23.3	11.4	0.47	9.2	11.9	8.42	11.8	0.639	19.4	8.5	0.47	10.3
13.4	9.52	11.9	0.639	23.3	11.4	0.47	9.1	12	8.55	11.9	0.639	19.2	8.6	0.47	10.4
13.4	9.49	11.9	0.639	23.2	11.3	0.47	9.1	12	8.45	11.9	0.639	19	8.5	0.47	10.5
13.4	9.49	11.9	0.639	23.2	11.3	0.47	9.1	12	8.45	12	0.639	18.9	8.5	0.47	10.6
13.4	9.49	11.8	0.639	23.2	11.3	0.47	9.0	12	8.44	12	0.639	18.7	8.4	0.47	10.7
13.4	9.49	11.8	0.639	23.2	11.3	0.47	9.0	12.1	8.43	12.1	0.639	18.5	8.4	0.47	10.8
13.4	9.49	11.9	0.639	23.2	11.3	0.47	9.1	12.1	8.57	12.1	0.639	18.4	8.6	0.47	10.8
13.3	9.46	11.8	0.639	23.2	11.2	0.47	9.0	12.1	8.57	12.1	0.639	18.3	8.6	0.47	10.9
13.9	9.84	12.4	0.639	23.5	11.5	0.52	9.4	12.4	7.24	12.2	0.639	19.9	7.2	0.52	10.6
13.9	9.8	12.4	0.639	23.4	11.4	0.52	9.4	12.5	7.21	12.3	0.639	19.9	7.2	0.52	10.7
13.9	9.78	12.3	0.639	23.4	11.4	0.52	9.3	12.5	7.27	12.3	0.639	19.9	7.3	0.52	10.7
13.9	9.78	12.3	0.639	23.4	11.4	0.52	9.3	12.6	7.31	12.5	0.639	19.9	7.3	0.52	10.9
13.8	9.76	12.3	0.639	23.4	11.4	0.52	9.3	12.6	7.25	12.6	0.639	19.8	7.3	0.52	11.0
13.9	9.78	12.3	0.639	23.4	11.4	0.52	9.3	12.6	7.29	12.6	0.639	19.8	7.3	0.52	11.0
13.9	9.78	12.3	0.639	23.4	11.4	0.52	9.3	12.7	7.31	12.7	0.639	19.9	7.3	0.52	11.1
13.8	9.77	12.3	0.639	23.3	11.4	0.52	9.3	12.8	7.22	12.7	0.639	19.8	7.2	0.52	11.2
13.8	9.74	12.2	0.639	23.3	11.4	0.52	9.2	12.9	7.27	12.8	0.639	19.8	7.3	0.52	11.3
14.2	9.97	12.6	0.639	23.6	11.3	0.58	9.5	13.1	7.3	13	0.639	20.1	7.3	0.58	11.3
14.2	9.96	12.6	0.639	23.6	11.2	0.58	9.5	12.8	7.28	12.5	0.639	20.1	7.3	0.58	10.7
14.3	9.98	12.6	0.639	23.6	11.3	0.58	9.5	12.7	7.27	12.4	0.639	20	7.3	0.58	10.6
14.3	9.99	12.6	0.639	23.6	11.3	0.58	9.5	12.5	7.24	12.2	0.639	20	7.2	0.58	10.4
14.3	9.98	12.6	0.639	23.6	11.3	0.58	9.5	12.5	7.25	12.1	0.639	20	7.3	0.58	10.3
14.3	9.99	12.6	0.639	23.6	11.3	0.58	9.5	12.4	7.27	12	0.639	20	7.3	0.58	10.2
14.3	9.98	12.6	0.639	23.6	11.3	0.58	9.5	12.4	7.3	12	0.639	20	7.3	0.58	10.1
14.2	9.97	12.6	0.639	23.5	11.3	0.58	9.5	12.3	7.22	11.9	0.639	20	7.2	0.58	10.0
14.2	9.98	12.6	0.639	23.5	11.3	0.58	9.5	12.2	7.27	11.8	0.639	20	7.3	0.58	9.9
14.6	10.2	12.9	0.639	23.6	11.3	0.63	9.7	12.8	7.36	12.3	0.639	20.4	7.4	0.63	10.3
14.6	10.1	12.8	0.639	23.6	11.3	0.63	9.7	12.7	7.36	12.2	0.639	20.4	7.4	0.63	10.2
14.6	10.2	12.9	0.639	23.6	11.4	0.63	9.7	12.7	7.29	12.1	0.639	20.4	7.3	0.63	10.1
14.6	10.2	12.9	0.639	23.6	11.4	0.63	9.7	12.6	7.27	12.1	0.639	20.4	7.3	0.63	10.0
14.6	10.1	12.8	0.639	23.6	11.3	0.63	9.6	12.6	7.3	12.1	0.639	20.4	7.3	0.63	10.0

Appendix: Experimental Data (*Continued*)

T_{ao}, °C	w_{ao}, g/kg da	T_{wo}, °C	$\dot{m}_w$, kg/s	T_{ai}, °C	w_{ai}, g/kg da	$\dot{m}_a$, kg/s	T_{wi}, °C	T_{ao}, °C	w_{ao}, g/kg da	T_{wo}, °C	$\dot{m}_w$, kg/s	T_{ai}, °C	w_{ai}, g/kg da	$\dot{m}_a$, kg/s	T_{wi}, °C
14.5	10.1	12.8	0.639	23.6	11.3	0.63	9.6	12.5	7.21	11.9	0.639	20.3	7.2	0.63	9.8
14.5	10.1	12.8	0.639	23.6	11.3	0.63	9.6	12.4	7.26	11.8	0.639	20.3	7.3	0.63	9.7
14.6	10.1	12.8	0.639	23.6	11.3	0.63	9.6	12.4	7.27	11.8	0.639	20.3	7.3	0.63	9.7
14.5	10.1	12.8	0.639	23.6	11.3	0.63	9.6	12.4	7.3	11.7	0.639	20.3	7.3	0.63	9.6
14.8	10.3	12.9	0.639	23.4	11.3	0.69	9.7	12.8	7.21	12	0.639	20.5	7.2	0.69	9.8
14.8	10.2	12.9	0.639	23.4	11.2	0.69	9.7	12.8	7.13	12	0.639	20.5	7.1	0.69	9.8
14.8	10.3	12.9	0.639	23.5	11.3	0.69	9.7	12.8	7.15	11.9	0.639	20.5	7.1	0.69	9.7
14.8	10.3	12.9	0.639	23.5	11.3	0.69	9.7	12.7	7.21	11.8	0.639	20.5	7.2	0.69	9.5
14.8	10.3	12.9	0.639	23.5	11.3	0.69	9.7	13	7.29	12.4	0.639	20.5	7.3	0.69	10.2
14.7	10.2	12.8	0.639	23.4	11.2	0.69	9.6	13.1	7.23	12.4	0.639	20.5	7.2	0.69	10.3
14.9	10.3	12.9	0.639	23.5	11.4	0.69	9.6	13.2	7.27	12.6	0.639	20.5	7.3	0.69	10.5
14.9	10.3	13	0.639	23.5	11.3	0.69	9.7	13.2	7.14	12.7	0.639	20.4	7.1	0.69	10.6
14.8	10.3	12.9	0.639	23.5	11.3	0.69	9.7	13.3	7.17	12.8	0.639	20.4	7.2	0.69	10.7
14.9	10.3	12.7	0.639	23.1	11.2	0.75	9.4	13.4	7.07	12.6	0.639	20.7	7.1	0.75	10.3
14.8	10.2	12.7	0.639	23	11.1	0.75	9.4	13.3	7.02	12.5	0.639	20.7	7.0	0.75	10.2
14.8	10.2	12.7	0.639	23	11.1	0.75	9.4	13.3	6.93	12.4	0.639	20.7	6.9	0.75	10.1
14.8	10.2	12.8	0.639	23	11.1	0.75	9.5	13.2	6.95	12.3	0.639	20.6	6.9	0.75	10.0
14.8	10.2	12.7	0.639	23	11.1	0.75	9.4	13.2	6.96	12.2	0.639	20.6	7.0	0.75	9.9
14.8	10.2	12.7	0.639	23	11.1	0.75	9.4	13.1	6.98	12.2	0.639	20.6	7.0	0.75	9.8
14.8	10.2	12.7	0.639	23	11.1	0.75	9.5	13.1	7.03	12.1	0.639	20.6	7.0	0.75	9.7
14.8	10.2	12.7	0.639	23	11.1	0.75	9.4	13.2	7.09	12.3	0.639	20.6	7.1	0.75	10.0
14.8	10.2	12.7	0.639	23	11.1	0.75	9.4	13.4	7.06	12.7	0.639	20.6	7.1	0.75	10.4
15.1	10.4	12.7	0.639	23.2	11.3	0.80	9.2	13.5	6.97	12.3	0.639	21	7.0	0.80	9.8
15.2	10.5	12.8	0.639	23.3	11.4	0.80	9.3	13.4	7.01	12.2	0.639	21	7.0	0.80	9.7
15.2	10.5	12.8	0.639	23.3	11.4	0.80	9.3	13.5	7.08	12.3	0.639	21	7.1	0.80	9.8
15.1	10.4	12.7	0.639	23.2	11.3	0.80	9.3	13.4	7.08	12.2	0.639	21	7.1	0.80	9.7
15.1	10.4	12.8	0.639	23.2	11.3	0.80	9.3	13.3	7.00	12.1	0.639	21	7.0	0.80	9.5
15.1	10.4	12.7	0.639	23.2	11.3	0.80	9.3	13.3	6.87	12.1	0.639	21	6.9	0.80	9.5
15.2	10.4	12.8	0.639	23.2	11.3	0.80	9.4	13.6	6.95	12.7	0.639	21	7.0	0.80	10.2
15.1	10.4	12.7	0.639	23.1	11.2	0.80	9.3	13.7	6.98	12.8	0.639	21	7.0	0.80	10.3
15.1	10.4	12.8	0.639	23.1	11.2	0.80	9.4	13.7	6.94	12.8	0.639	20.9	6.9	0.80	10.4
15.0	10.3	12.3	0.639	22.5	11.2	0.85	8.8	13.9	7.03	12.8	0.639	21.1	7.0	0.85	10.2
15.1	10.4	12.3	0.639	22.7	11.3	0.85	8.8	13.8	7.03	12.7	0.639	21	7.0	0.85	10.1
15.0	10.3	12.3	0.639	22.8	11.2	0.85	8.8	13.8	7.09	12.6	0.639	21.1	7.1	0.85	10.0
15.1	10.4	12.4	0.639	22.9	11.1	0.85	8.9	13.8	7.06	12.6	0.639	21.1	7.1	0.85	10.0
15.1	10.4	12.4	0.639	23	11.2	0.85	8.9	13.7	6.99	12.5	0.639	21.1	7.0	0.85	9.9
15.1	10.4	12.5	0.639	23	11.2	0.85	9.0	13.7	6.99	12.5	0.639	21.1	7.0	0.85	9.9
15.2	10.4	12.5	0.639	23.1	11.2	0.85	9.0	13.7	7.01	12.4	0.639	21.1	7.0	0.85	9.8
15.1	10.4	12.5	0.639	23.1	11.1	0.85	9.0	13.7	7.07	12.4	0.639	21.1	7.1	0.85	9.7
15.2	10.4	12.5	0.639	23.1	11.2	0.85	9.0	13.7	7.06	12.4	0.639	21.1	7.1	0.85	9.7
11.3	8.32	11.3	0.639	17.6	8.8	0.30	10.4								